



# Estimation of the heat required for intermediate pyrolysis of biomass

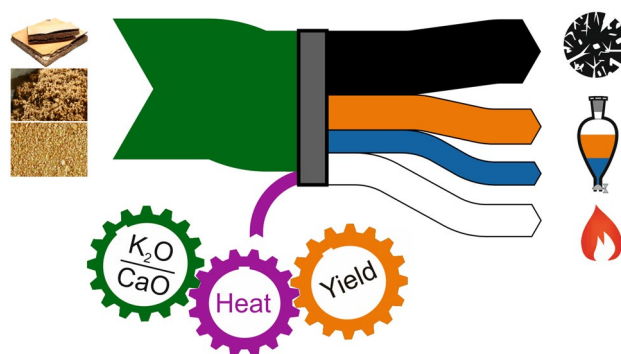
Wojciech Jerzak<sup>1</sup> · Markus Reinmüller<sup>2,3</sup> · Aneta Magdziarz<sup>1</sup>

Received: 10 December 2021 / Accepted: 20 August 2022 / Published online: 2 September 2022  
© The Author(s) 2022

## Abstract

Biomass waste contains an abundant source of energy that can be transformed into high-calorific fuel during intermediate pyrolysis, consequently reducing the use of fossil fuel resources. In the present study, medium density fibreboard (MDF), brewery spent grains (BSG) and post-extraction soybean meal (SM) were used to pyrolysis. Valorisation of these wastes via intermediate pyrolysis was carried out at a temperature of 773 K in a fixed-bed reactor under nitrogen atmosphere. The ultimate analysis showed that MDF char has offered the highest carbon content. Generally, chars obtained from these feedstocks were characterized by different internal microstructures. On the one hand, the surface of MDF char has exhibited pores with a regular pattern of small perpendicular blocks. On the other hand, irregular open spaces were detected in BSG and SM chars. The results of this investigation of the microstructure proved that the studied biomass wastes are perspective feedstocks to obtain high-value bioenergy products. Based on the enthalpy balance, it was concluded that the heating value of the pyrolysis gas was higher, the more endothermic pyrolysis process. The research hypothesis confirms that the higher the  $K_2O/CaO$  ratio in the ash, the better biomass pyrolysis process was catalysed and as a result, less additional heat was required for pyrolysis. To carry out the pyrolysis of MDF, SM and BSG, additional heat input was required in the amount of 2016.8, 1467.9 and 881.1 kJ, respectively. It was found that 4–10% of the higher heating value of the raw materials was missing to achieve the self-sustaining energy of intermediate pyrolysis.

## Graphical abstract



**Keywords** Biomass · Valorisation · Pyrolysis · Thermogravimetric analysis · Enthalpy balance · Fourier transform infrared spectroscopy

## Introduction

Plants for the thermal conversion of biomass waste to fuel have an increasing importance nowadays, in particular when these are installed near the waste generation sites. The problem of feedstocks transport of especially with low energy

✉ Wojciech Jerzak  
wjerzak@agh.edu.pl

Extended author information available on the last page of the article

density is eliminated, as well as the associated additional fuel consumption and emission of pollutants to the environment. One of the promising thermal technologies promoting the conversion of the feedstocks from waste to energy is pyrolysis. Today, many types of fast (Bridgwater 2012), intermediate (Funke et al. 2017), and slow (Cong et al. 2018) pyrolysis reactors have been developed. Recently, Yang et al. (2021) reported that intermediate pyrolysis may be an alternative to fast and slow pyrolysis. Biochar is the main product of slow pyrolysis characterized by a low heating rate, while maximization of bio-oil is achieved at high sample heating rates (1000 K/s) in fast pyrolysis (Bertero and Sedran 2015). On the other hand, moderate heating rates (100–500 K/min) are used in intermediate pyrolysis (Hornung 2013), which favours the production of approximately 40 wt% of char and 40 wt% of bio-oil (Bridgwater 2018).

Fast pyrolysis technologies face several challenges that must be resolved. First of all, the feedstock for fast pyrolysis should have a small particle size (1–2 mm) due to the required heat transfer and material transport (Mašek 2016). However, fluidized bed reactors operating on a laboratory scale require particles less than 500  $\mu\text{m}$  (Morgan and Kandiyoti 2014), and sometimes even less than 120  $\mu\text{m}$  (Bertero and Sedran 2015). Biomass has low thermal conductivity and only small particle sizes can provide the high heating rate necessary for fast pyrolysis. Another problem is bio-oil with a high content of oxygen, water and high acidity (Chong et al. 2019). For this reason, catalytic upgrading of pyrolytic oil is recommended (Mohammed et al. 2017b). Furthermore, fast pyrolysis char offers a sticky nature and these are fine particles that tend to end up in liquid products (Bridgwater 2018). The above-mentioned challenges resulted in the intensive development of the intermediate pyrolysis. Intermediate pyrolysis liquid products have evidently featured lower tar contents and may be suitable for direct use in boilers in contrast to fast pyrolysis (Mahmood et al. 2013).

Herein, it was found that the ash content of the feedstock influenced on the intermediate pyrolysis yield. Higher yields of oils obtained from intermediate pyrolysis were observed when the ash content in the feedstocks increases (Funke et al. 2017). Even a very low ash content (0.5 wt%) added to cellulose can dramatically improve the yield of compounds with lower molecular weight (in particular, formic acid, glycolaldehyde, and acetol) (Patwardhan et al. 2010). Potassium and sodium are known for their strong catalytic activity, whereas calcium and magnesium catalyse the pyrolysis reactions to a moderate extent. Magnesium, which was added to the feedstock in the form of  $\text{MgCl}_2$  or  $\text{Mg}(\text{NO}_3)_2$ , promotes the formation of the pore structure in the char and reduces the CO yield and at the same time increases the  $\text{CO}_2$  yield (Zhang et al. 2020). A high ash content in the feedstock promotes catalytic pyrolysis reactions and reduces the effect

of the pyrolysis temperature on particular yields (Hoekstra et al. 2012). The increase in the ash content of the feedstock corresponds to a higher solid yield as an inert material and promotes repolymerization reactions (Funke et al. 2017). Notably, a high ash content promotes carbon retention in the biochar. Not only the ash content affects the pyrolysis products yield but also the ash composition in the feedstock. Ash, mainly alkali metals from nutrients in biomass, catalyses reactions in fast pyrolysis vapours (Bridgwater 2018). However, the current number of studies on the influence of ash composition on the product yield from intermediate pyrolysis is very limited (Mohammed et al. 2016a). The catalytic activities of silica and potassium in ash were assigned to the reduction of acids, aldehydes, and ketones in oils (Mohammed et al. 2017c). Ashes that are rich in silicon and aluminium reduce the aqueous phase in the oil and improve the yield of non-condensing gas (Mohammed et al. 2016a).

To compare the operation conditions of different pyrolysis reactors, the required heat input of the process must be determined. Generally, the heat required for the pyrolysis process depends on many factors, e.g. temperature, reactor design, catalyst application, heating rate, heat transport, pressure, biomass type, particle size, solid and vapour residence time, etc. By using various methods to determine the required heat for pyrolysis, a large variation in the reported values (from exothermic to endothermic) has been obtained in the literature (Hosokai et al. 2016). The exothermic effects of the pyrolysis reaction were typically detected by differential scanning calorimetry (DSC) (Gomez et al. 2009). This method has been successfully applied for slow pyrolysis studies. Applying the DSC method confirmed that the exothermic effect was caused by secondary pyrolysis reactions (Chen et al. 2014). The exothermic effect was also observed on the basis of laboratory experiments (Kodera and Kaiho 2016) as well as for the primary stage of hemicellulose and lignin pyrolysis (Yang et al. 2007). An endothermic effect of slow pyrolysis has been reported based on experimental studies carried out in a fixed bed reactor (Ábrego et al. 2019) and a screw conveyor pyrolysis reactor (Cong et al. 2018). Comparing the results for biomass pyrolysis at 823 K, the additional heat required was 0.55 MJ/kg for the fixed-bed reactor, and 2.30 MJ/kg for the screw conveyor pyrolysis reactor. On the other hand, fast pyrolysis of biomass also required an additional energy supply. The total heat required for fast pyrolysis ( $T = 823 \text{ K}$ ) of different biomasses was 1.30–1.60 MJ/kg of dry feedstocks (Daugaard and Brown 2003). An extra heat transfer to the carrier gas, i.e. nitrogen, in the order of 1.6 MJ/kg feedstock has to be considered (Fonts et al. 2021). Including the heating of nitrogen used as a carrier gas, the total heat required for fast pyrolysis was 3 MJ/kg. There is an entire lack of literature on the values of the heat required for intermediate pyrolysis.

This paper presents an analysis of the pyrolysis products and yields in relation to an in-depth investigation of feedstocks. This kind of analysis of raw materials includes the ash content, the ash composition, the determination of the cellulose, hemicellulose, and lignin fibre content, and identifies the functional groups of the organic compounds. The necessary knowledge in this field still requires further investigation because a few studies were reported only for the fast and slow pyrolysis process. The ash content and composition of the feedstock used in intermediate pyrolysis may play a more important role than in the case of fast pyrolysis because of the longer vapour residence times of the feedstock in the reactor. In consequence, the results of this study will fill the knowledge gap and contribute to a better understanding how the feedstocks composition affects the pyrolysis products. As mentioned above, the potassium-rich and calcium-poor biomass ash shows a strong catalytic effect on the pyrolysis process. Therefore, the hypothesis was proposed that the lower the  $K_2O/CaO$  ratio in the biomass ash, the less heat may be required for the pyrolysis process. Finally, an enthalpy balance was established to determine the heat required for intermediate pyrolysis, as the literature lacks results considering the heat balance for intermediate pyrolysis.

## Materials and methods

Three biomass wastes were selected for this study: medium density fibreboard (MDF), brewery spent grains (BSG) and post-extraction soybean meal (SM). The above-mentioned biomass wastes are by-products from the wood, brewery and food agricultural industries, respectively. All feedstocks were prepared for the experiments, including drying under ambient conditions and sieving of the particles to particle sizes of 300–750  $\mu\text{m}$ .

### Measurement methods and instruments

The moisture content of feedstocks was determined in a laboratory dryer using the standard PN-EN ISO 18134-2:2017-03. The samples were dried at a temperature of 378 K in an air atmosphere until a constant mass was achieved. The ash content was determined in a muffle furnace according to the standard PN-EN ISO 18122:2016-01, where the ash content was calculated based on the mass of the residue remaining after the sample was heated under air at a controlled temperature of  $823 \pm 10$  K. The volatile matter content was determined on PN-EN ISO 18123:2016-01. A Truspec CHNS 628 Leco (USA) analyser was employed for the analysis of the main organic elements. The chemical composition of the ash was determined by X-ray fluorescence (XRF) analysis applying a WD-XRF ZSX Primus II

Rigaku spectrometer (Rh lamp) equipment from company Rigaku, Japan. A fibre analysis of feedstocks was determined using the Van Soest method (Van Soest 1963) to obtain the content of cellulose, hemicellulose, and lignin. Fibre analysis (NDF, neutral detergent fraction; ADF, acid detergent fraction, and ADL, acid detergent lignin) was performed with neutral and acidic detergents. Fourier transform infrared spectroscopy (FTIR) was employed to identify the functional groups of the organic compounds in feedstocks using a Bruker Alpha II system from Bruker Optics Inc., USA. The applied infrared absorption frequency has covered the range of 400–4000  $\text{cm}^{-1}$ . Raw materials thermogravimetric analysis (TGA) was performed with a Mettler Toledo TGA/SDTA 851 apparatus (Schwarzenbach, Switzerland). The TGA measurements were made with a nitrogen gas flow of 40 ml/min. Approximately 5 mg of each sample in an aluminium crucible were heated from 298 to 773 K at a heating rate of 10 K/min. Subsequently, the sample was kept at a constant temperature of 773 K for 7 min to replicate the experimental conditions in the fixed-bed reactor. Finally, an analysis of the pyrolysis products (char, oil, and aqueous phase) was performed. Pyrolysis gases were collected in gasbags and quantified by gas chromatography. The morphology and structure of the obtained chars were determined using scanning electron microscopy (SEM) of the type Inspect S50 apparatus from FEI, USA. SEM images were collected using a secondary electron detector in the high-vacuum mode at an applied acceleration voltage of 3 keV.

### Pyrolysis in a fixed-bed reactor

The implementation of intermediate pyrolysis of biomass with particle sizes below 750  $\mu\text{m}$  is a challenge to perform in Auger-type reactors. This originates from the van der Waals forces, electrostatic forces and capillary forces leading to agglomeration between the particles and adhesion of the particles to the walls. As a result, the feedstock is compacted and the release of volatile parts is limited. For this reason, the use of the fixed-bed reactor for the intermediate pyrolysis of biomass with a particle diameter of less than 750  $\mu\text{m}$  is justified. The pyrolysis process was performed in a fixed-bed reactor electrically heated to 773 K. The sample was placed in a boat into the zone of the water cooler and the reactor was purged with nitrogen at a flow rate of 100 ml/min for five minutes. The main process of intermediate pyrolysis has started with the insertion of the boat with the sample into the heated furnace. The residence time of the sample in the furnace was seven minutes, and that of the vapours in the hot zone was twenty seconds. After the pyrolysis was complete, the sample boat was moved back to the fast water-cooler zone. The process of purging the reactor with nitrogen, pyrolysis of 3 g of sample, and cooling took in total 30 min. Therefore, the theoretical time required to pyrolyze 1 kg of

feedstock in this laboratory stand was 166.67 h. As a result, each 3 g sample was pyrolyzed every 23 min. Naturally, the performance of an up-scale intermediate pyrolysis experiment will ensure continuous feed, and the time required for pyrolysis will be minimized. The respective ratio of nitrogen required for the pyrolysis was  $1.145 \frac{\text{kgN}_2}{\text{kgfeedstock}}$ . The temperature of the sample was monitored using a K-type thermocouple. The gaseous pyrolysis produced has passed through an ice tank, where the aqueous and oil phases were condensed. A gravimetric tool was used to separate the aqueous phases and oil. More details concerning the experimental stand can be found in our previous work (Jerzak et al. 2022).

### Procedure for determining the heat of pyrolysis

The heat required or emitted from biomass waste pyrolysis ( $Q_{py}$ ) is defined as the difference between enthalpy outflow ( $H_{out}$ ) and inflow ( $H_{in}$ ) by the following equation:

$$Q_{py} = H_{out} - H_{in}. \quad (1)$$

The enthalpy balance of the pyrolysis reactor is illustrated in Fig. 1.

The inflow of enthalpy under the reference conditions ( $T_{in} = 298 \text{ K}$ , 1 atm) includes:  $H_{N_2,in}$ —the enthalpy from the nitrogen flowing into the system and  $H_{feed}$ —enthalpy of feedstock.

$$H_{in} = H_{feed} + H_{N_2,in}, \quad (2)$$

$$H_{feed} = H_{feed}^0 + \Delta H_{feed}. \quad (3)$$

$H_{feed}^0$  – is the standard enthalpy of feedstock (kJ/kg).

$$H_{feed}^0 = \nu_i \cdot H_{f,CO_2}^0 + \nu_j \cdot H_{f,H_2O}^0 + HHV, \quad (4)$$

where  $\nu_i, \nu_j, H_{f,CO_2}^0, H_{f,H_2O}^0$  are the stoichiometric coefficients and enthalpies of formation of  $CO_2$  and  $H_2O$ , respectively.

The higher heating value (HHV) of the compound can be calculated under reference conditions (298 K, 1 atm) from the equation of Channiwala and Parikh (2002),

$$HHV = 349.1 \cdot C + 1178.3 \cdot H + 100.5 \cdot S - 103.4 \cdot O - 15.1 \cdot N - 21.1 \cdot A \quad (\text{in kJ/kg}), \quad (5)$$

where C, H, S, O, N, and A are the mass percentages of carbon, hydrogen, sulphur, oxygen, nitrogen, and ash based on the dry mass of the feedstock, char, oils with tars, and aqueous phase.

At a temperature of 298 K, the values can be defined as  $\Delta H_{feed} = 0$  and  $H_{N_2,in} = 0$  (Yang et al. 2013).

However, the enthalpy outflow at the reference conditions ( $T_{out} = 773 \text{ K}$ , 1 atm) includes the enthalpies of nitrogen, char, oils with tar, aqueous phase, and pyrolysis gas (index gas):

$$H_{out} = H_{N_2,out} + H_{char} + H_{oil} + H_{aq. phase} + H_{gas} \quad (6)$$

The enthalpy of nitrogen in the outflow was calculated as follows:

$$H_{N_2,out} = \dot{m}_{N_2} \cdot \int_{T_{in}}^{T_{out}} \bar{C}_{p,N_2}(T) dT, \quad (7)$$

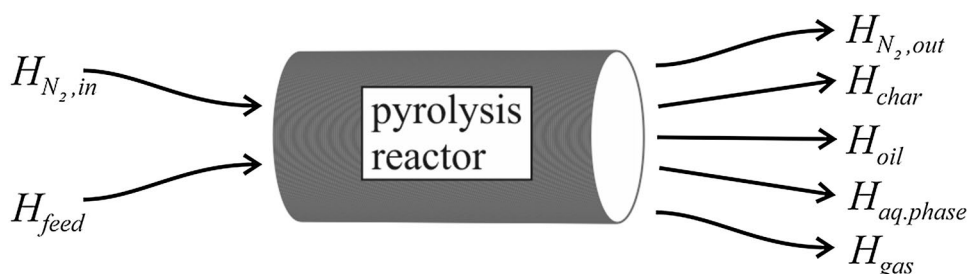
where  $\dot{m}_{N_2}$  – is mass flow rate of nitrogen per feedstock mass,  $\bar{C}_{p,N_2}(T)$  – the average specific heat of nitrogen in the temperature range of 298–773 K. This value was calculated from the polynomial in Eq. (6) given in  $\frac{J}{\text{mol}\cdot\text{K}}$  (Linstrom, PJ. and Mallard, WG. 2003) and converted into  $\frac{J}{\text{kg}\cdot\text{K}}$ .

$$C_{p,N_2}(T) = 17.071 + 1.739 \cdot 10^{-3} \cdot T - 230154.97 \cdot T^{-2} - 4.518 \cdot 10^{-6} \cdot T^2 + 2939.805 \cdot T^{-1} \quad (8)$$

The enthalpies of char, oil, aqueous phase, and pyrolysis gas are expressed in Eqs. (9), (10), (11) and (12), respectively. The enthalpies for each of the pyrolysis products (char, oil, aqueous phase, and pyrolysis gas) are the sum of the standard enthalpy of formation at 298 K and the amount of heat required for increasing the temperature from 298 to 773 K.

$$H_{char} = H_{char}^0 + \Delta H_{char} = H_{char}^0 + \dot{m}_{char} \cdot \bar{C}_{p,char}(T_{out} - T_{in}), \quad (9)$$

**Fig. 1** A simplified scheme for the estimation of the enthalpy balance



$$\begin{aligned}
 H_{oil} &= H_{oil}^0 + \Delta H_{oil} \\
 &= H_{oil}^0 + \dot{m}_{oil} \cdot \bar{C}_{p,oil}(T_{out} - T_{in}),
 \end{aligned}
 \tag{10}$$

$$\begin{aligned}
 H_{aq,phase} &= H_{aq,phase}^0 + \Delta H_{aq,phase} \\
 &= H_{aq,phase}^0 + \dot{m}_{aq,phase} \cdot \bar{C}_{p,aq,phase}(T_{out} - T_{in}),
 \end{aligned}
 \tag{11}$$

$$\begin{aligned}
 H_{gas} &= H_{gas}^0 + \Delta H_{gas} \\
 &= H_{gas}^0 + \dot{m}_{gas} \cdot \bar{C}_{p,gas}(T_{out} - T_{in}).
 \end{aligned}
 \tag{12}$$

The standard enthalpy of char, oil, and aqueous phase can be calculated analogously to feedstocks (Eq. 4) with the use of HHV (Channiwala and Parikh 2002). These calculations have used the correlations of the average specific heat capacity of char from Haseli et al. (2011), oil from Atsonios et al. (2015), and the aqueous phase. At a temperature of 773 K, the aqueous phase and the oil were considered as gas vapours.

For pyrolysis gases, the standard enthalpy was described as follows:

$$H_{gas}^0 = \sum_{k=1}^n x_k \cdot H_{f,k}^0,
 \tag{13}$$

where  $x_k$  – mole fraction of pyrolysis gas component,  $H_{f,k}^0$  – standard enthalpy of formation gaseous species (Linstrom, PJ. and Mallard, WG. 2003), and  $n$  – the total number of compounds involved in the pyrolysis gas.

## Results and discussion

The biomass waste selected for this research was produced in Poland. However, the exact localization of biomass waste generation does not fundamentally influence of the main components, as verified by the results of other MDF (Couret et al. 2017), BSG (Xiros et al. 2008), and SM (Oliveira et al. 2015).

### Feedstock characteristics

Table 1 lists the component analysis of the investigated feedstocks. The highest content of hemicellulose was found in BSG, whereas in MDF cellulose was the dominant component. The high amount of cellulose in MDF (around 40 wt%) was confirmed by Couret et al. (2017). Other studies (Xiros et al. 2008) have outlined that the composition of BSG was very variable and depends on period of harvest, barley variety, malting and mashing conditions. They found that BSG can contain certain ranges of 9–25 wt% cellulose, 19–40 wt% hemicellulose, and 4–20 wt% lignin. As expected, low contents of cellulose, hemicellulose, and lignin were detected in

**Table 1** Component analysis of the studied feedstocks

Component	MDF	BSG	SM
cellulose <sup>a</sup> (wt%)	45.43	13.49	2.71
hemicellulose <sup>a</sup> (wt%)	23.67	46.02	5.26
lignin <sup>a</sup> (wt%)	16.29	1.39	0.05
extractives <sup>a</sup> (wt%)	14.61	39.10	91.98

<sup>a</sup>Dry and ash free

SM, because the protein content of SM can be as high as 53.5 to 56.2 wt% moisture-free basis (Grieshop et al. 2003).

In the next step, MDF, BSG, and SM were characterized by applied thermogravimetric analysis. Figure 2 shows the thermogravimetric and derivative (TG/DTG) curves with a time change during the pyrolysis of MDF, BSG and SM. The most significant mass losses were observed in the temperature range: 538–660 K (MDF), 528–740 K (BSG), 498–743 K (SM). In these temperature ranges, the maximum degradation of main components of the biomass (DTG<sub>max</sub>) occurred at 627.1, 578.7, and 592.8 K for MDS, BSG, and SM, respectively. MDF was rich in cellulose, and the sharp peak of DTG seen in Fig. 2a was attributed to cellulose decomposition (Chen et al. 2022). In turn, the DTG shoulder peaks shown in Fig. 2b and c were attributed to degraded hemicelluloses and the decomposition of the soy protein backbone, respectively (Chen et al. 2020). The mass of char was determined not only by the process temperature but also by the holding time of char at a constant temperature (the area marked in green in Figs. 2a–c). Holding the chars at 773 K for seven minutes lowered their weight by 1.2–1.4 wt%. After pyrolysis, most of the char was formed from SM (35.26 wt%) and the least from BSG (22.21 wt%).

Table 2 demonstrates that MDF, BSG, and SM are characterized by a low moisture content as they have been previously dried. Among the feedstocks examined, SM was distinguished by a comparably high ash content of 9.91 wt% (as much as seven times more than MDF and BSG). BSG has offered the highest HHV of 21.28 MJ/kg, which results from the highest carbon and hydrogen contents as well as the lowest oxygen amount of all three feedstocks. Each of the feedstocks was additionally characterized by a low sulphur content.

One of the indices enabling the assessment of feedstocks for pyrolysis is the effective molar ratio of hydrogen to carbon ((H/C)<sub>eff</sub>) (Chen et al. 1988):

$$\left(\frac{H}{C}\right)_{eff} = \frac{H - 2O}{C},
 \tag{14}$$

where H, C, and O are the absolute numbers of atoms of hydrogen, carbon, and oxygen, respectively. Using (H/C)<sub>eff</sub>, it can be determined if a pyrolysis feedstock has sufficient



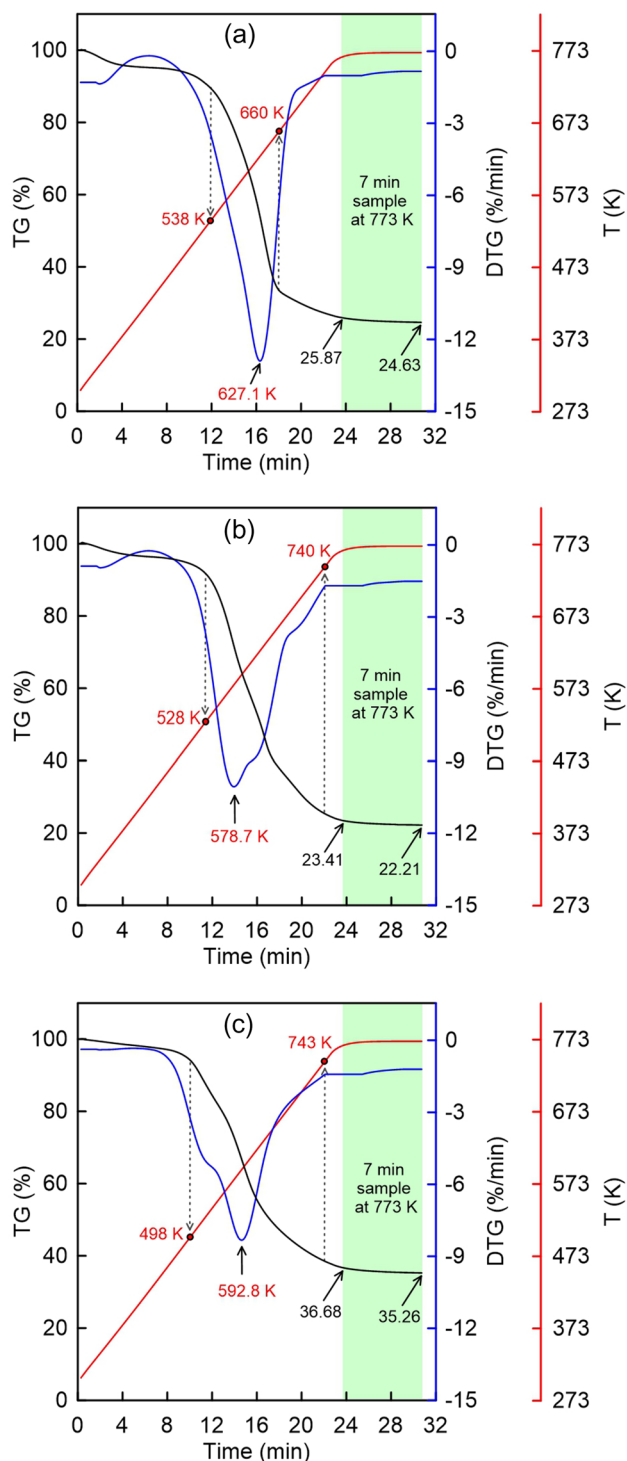


**Fig. 2** Thermal behaviour curves (TG/DTG) during the pyrolysis of biomass: **a** MDF, **b** BSG, and **c** SM

hydrogen to form the desired aromatics and if the feedstock will result in excessive coke generation.

The ratio  $(H/C)_{\text{eff}}$  of the biomass wastes typically ranges from 0 to 0.35 (Wang et al. 2020). Biomass feedstocks with a lower  $(H/C)_{\text{eff}}$  ratio are known to have lower thermal

**Table 2** Proximate analysis, ultimate analysis, resulting elemental ratios, and heating value of the studied feedstocks

Parameter	MDF	BSG	SM
Moisture <sup>a</sup> (wt%)	1.70	2.68	3.24
Volatile matter <sup>b</sup> (wt%)	81.86	86.15	79.28
Ash <sup>b</sup> (wt%)	1.37	1.42	9.91
Fixed carbon (wt%) <sup>c</sup>	15.07	9.75	7.57
C <sup>b</sup> (wt%)	45.59	48.70	39.44
H <sup>b</sup> (wt%)	6.84	7.18	5.94
N <sup>b</sup> (wt%)	4.91	4.07	6.75
S <sup>b</sup> (wt%)	0.05	0.26	0.17
O <sup>d</sup> (wt%)	42.60	39.80	47.71
H/C molar ratio	1.79	1.76	1.80
O/C molar ratio	0.70	0.61	0.91
N/C molar ratio $\times 10^{-2}$	9.24	7.16	14.67
Empirical formula	CH <sub>1.79</sub> O <sub>0.70</sub>	CH <sub>1.76</sub> O <sub>0.61</sub>	CH <sub>1.80</sub> O <sub>0.91</sub>
Formula weight (g/mol)	25.03	23.60	28.35
HHV (kJ/g)	19.47	21.28	15.54

<sup>a</sup>As received,

<sup>b</sup>Dry basis,

<sup>c</sup>Fixed carbon = 100%—Moisture—Volatile matter—Ash,

<sup>d</sup>By difference

stability. As discussed in the literature (Zhang et al. 2011), biomass feedstocks with  $(H/C)_{\text{eff}} < 0.3$  index will produce more coke and less hydrocarbons in the pyrolysis process. The high amount of oxygen together with low carbon and hydrogen contents in SM results in  $(H/C)_{\text{eff}}$  ratio of  $-0.46$ . In turn,  $(H/C)_{\text{eff}}$  for MDF and BSG are 0.11 and 0.31, respectively. Based on this calculation, SM and MDF are favoured compared to BSG to produce the targeted fuels.

The chemical composition of the ashes contained in the investigated feedstocks is clearly different, as shown in Table 3. MDF ash is distinguished from other feedstocks by a high content of TiO<sub>2</sub> (22.3 wt%) and CaO (22.1 wt%). Typically, the content of TiO<sub>2</sub> in biomass ash does not exceed 1 wt%, except for shredded currency, which contains 27.6 wt% TiO<sub>2</sub> (Vassilev et al. 2010). The sources of the elements of titanium, iron, and chlorine detected in MDF ash are most likely finishing materials, i.e. paints and coatings, and additives of polyvinyl chloride (PVC), and traces left by locks, hinges, etc. installed in furniture. The main inorganic elements of BSG were phosphorus, potassium, magnesium, iron, and calcium. This ash contains almost 40 wt% of phosphorus oxide. In contrast, SM ash was mainly shaped by the two components CaO and K<sub>2</sub>O, and their sum covers nearly 75 wt%. As shown in Table 3, the ash contains a variable content of the oxides CaO and K<sub>2</sub>O. Compared to calcium, potassium has a strong catalytic effect. The calculated K<sub>2</sub>O/CaO ratios in BSG, SM, and MDF ash were 2.04, 0.87, and

**Table 3** Chemical composition of the ash of the biomasses studied determined by XRF analysis

Ash composition (wt%)			
Component	MDF	BSG	SM
Na <sub>2</sub> O	10.35	1.85	0.11
MgO	3.04	10.91	5.57
Al <sub>2</sub> O <sub>3</sub>	2.58	0.67	0.38
SiO <sub>2</sub>	6.67	4.37	1.09
P <sub>2</sub> O <sub>5</sub>	2.45	39.61	17.07
SO <sub>3</sub>	7.38	2.41	1.53
K <sub>2</sub> O	7.94	19.41	34.16
CaO	22.11	9.49	39.19
TiO <sub>2</sub>	22.27	0.06	0.04
MnO	1.25	0.25	0.09
Fe <sub>2</sub> O <sub>3</sub>	11.41	10.48	0.49
CuO	0.11	0.06	0.03
ZnO	0.99	0.31	0.07
SrO	0.07	0.04	0.08
PbO	0.11	0.02	0
Cl	1.14	0.01	0.05

0.36, respectively. A high value of the K<sub>2</sub>O/CaO ratio can favour the catalysis of the pyrolysis reaction.

Figure 3 shows the FTIR spectra of the three investigated feedstocks. The peaks of wavenumbers are labelled in Fig. 3 and are related to the different functional groups listed in Table 4. In Fig. 3a, the spectrum of microcrystalline cellulose purchased from Acros Organics is plotted in addition to MDF. All characteristic peaks for cellulose are in line with those for MDF. Generally, the O–H fingerprint stretching vibrations bends (around 3300 cm<sup>-1</sup>) and C–H stretching in methyl, and methylene groups (around 2900 cm<sup>-1</sup>) have appeared for all investigated feedstocks (Alper et al. 2015). Peak No. 1 corresponds not only to the moisture adsorbed and the urea–formaldehyde resin in the case of MDF (Zazycki et al. 2020), but also to amine groups (El-Hendawy 2006). The high of peak No. 1 has corresponded to the nitrogen content in the sample, i.e. the lowest contents and absorbance were detected for BSG and the highest one for SM. The FTIR spectrum for SM has indicated a significant difference in the wavenumber range from 1700–400 cm<sup>-1</sup> compared to MDF, BSG, and cellulose absorption bands. For SM, the relative intensities of the absorption bands are obviously increased compared to the others, which is due to the high protein content indicated by peaks No. 1, 4, and 6. Other peaks No. 9, 11, and 12 can be addressed to a combination of different types of vibrations, derived from the alcohols, phenols, and primary and secondary amides.

## Char morphology

The morphology and structure of the obtained chars are shown in Fig. 4. SEM analysis confirmed that each of the chars has a characteristic diversified structure. MDF char has offered an open and highly complex three-dimensional framework. The regular pattern of pores (with diameter ≤ 10 μm) are visible, where the vascular bundles (tracheids) of the wood clearly remain in the char after pyrolysis. Interestingly, the orderly arrangement of the pores in MDF char has not been reported in other types of pyrolysis reactors (e.g. Auger reactors) (Ferreira et al. 2015). In such kinds of studies, the char has contained a broken fibre structure and irregular surface, with cavities and cracks (Ferreira et al. 2015). Moreover, this high heating rate – in this study it was close to 200 K/min – favours the formation of large cavities in the chars (Dahou et al. 2021). In contrast to MDF, BSG char (Fig. 4b) has particles with irregular open spaces (even reaching sizes of approximately 150 μm) with mixed structure, i.e. flat and sponge-like elements with pores. It can be assumed that flat char structures may arise from the shell of the kernel or other structures, plant structures, while sponge-like structures may result from the kernel. These particles are heterogeneous compared to MDF char. By analysing the middle photographs of the char in Figs. 4b and c, large internal cavities and an open structure can be observed in both cases. Volatile substances are immediately released after transport to the surface at high heating rates. This can cause a significant internal overpressure and the coalescence of the smaller pores. A char with a similar appearance, i.e. irregularly shaped macro- and microparticles with a sponge-like structure, containing pores of various sizes and many empty channels, has been reported by Cancelliere et al. (2019). SM char is characterized by a sponge-like structure with white inclusions. These inclusions have appeared at the outer surface of the particle, and thus it can be assumed that these species are transferred from the interior to the outside of the particles or stick to the tar at the outside.

## Yield of pyrolysis products

The mass of the different groups of pyrolysis products, in particular, the generated tars, was determined by the weighing method. The aqueous phase was separated from the liquid phase by gravimetric settling. At the end of each experimental campaign involving the pyrolysis of 10 samples, the pipes containing the tar was removed from the system and weighted. The tar content for MDF, BSG and SM based on the feedstock input was 2.5, 3.6 and 4.8 wt%, respectively. Subsequently, the pipes were cleaned with acetone and the system was reassembled. A chemical composition of the tars has not been analysed due to the difficulties in collecting of the low masses. For the determination of the particular

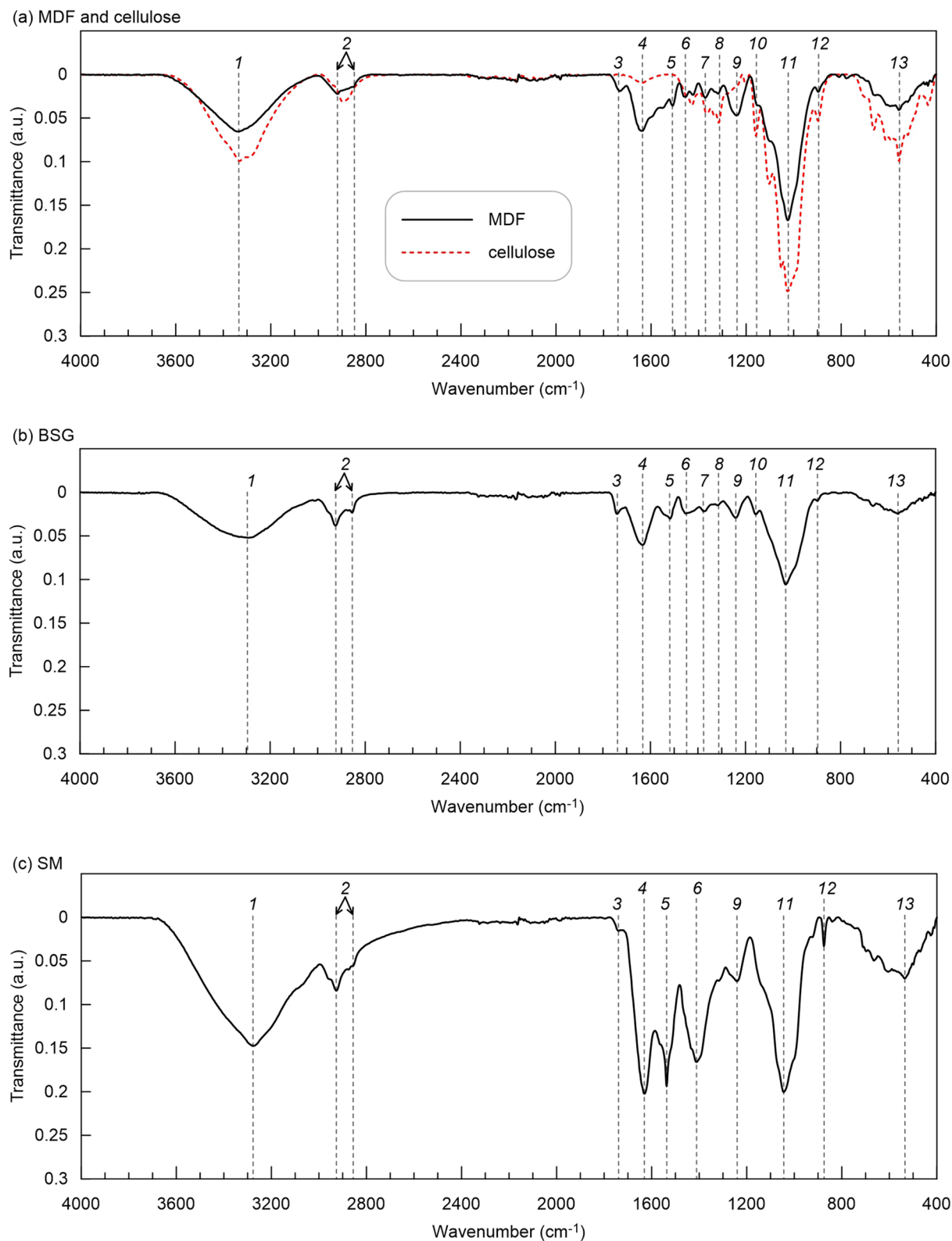


**Fig. 3** FTIR analyses of biomass: **a** MDF and cellulose, **b** BSG, and **c** SM



**Table 4** FTIR band assignments for waste biomass

Peak No.	Wavenumber (cm <sup>-1</sup> )			Band assignment	References
	MDF	BSG	SM		
1	3333	3294	3278	O–H and N–H stretching vibrations	(El-Hendawy 2006)
2	2921	2925	2927	C–H stretching in methyl, and methylene groups	(Alper et al. 2015)
	2853	2855	2874		
3	1730	1741	1739	C=O stretching in unconjugated ketone	(El-Hendawy 2006)
4	1638	1632	1632	C=O stretching and N–H bending vibrations	(El-Hendawy 2006)
5	1510	1518	1537	C–H aromatic skeletal vibrations	(Couret et al. 2017)
6	1457	1450	1411	N=O stretching in nitril	(Sun et al. 2021)
7	1372	1376	–	Aliphatic C–H stretching in methyl and phenol OH	(Gonultas and Candan 2018)
8	1316	1316	–	C–H vibration in cellulose and C–O vibration in syringyl derivatives	(Gonultas and Candan 2018)
9	1240	1242	1240	C–H and C–O stretching vibrations	(Pan and Jiang 2019)
10	1160	1158	–	C–O–C asymmetrical-stretching vibration	(Li et al. 2018)
11	1024	1033	1044	C–O, C=O, and C–H stretching vibrations	(Borel et al. 2018)
12	898	898	876	C–H and NO <sub>2</sub> bending	(El-Hendawy 2006)
13	558	558	534	C=O bending and C–H stretching vibrations	(Pan and Jiang 2019)

yields, the masses of the tar and oil fractions were treated as one group.

Based on the measurements of the mass of the different pyrolysis products, their yields were assessed. Figures 5a–c illustrate the pyrolysis product yields of the three feedstocks studied.

Finally, the yield of the gaseous product was obtained based on the following mass balance:

$$\text{Gas yield}(wt\%) = 100 - \text{char} - \text{aq. phase} - \text{oil and tars} \tag{15}$$

Considering the char, the highest yield (32.4 wt%) was obtained for SM. This result was in agreement with Sun et al. (2021) for similar pyrolysis conditions. Depending on the type of feedstock, the char yield in intermediate pyrolysis can reach 40 wt% (Bridgwater 2018). Furthermore, as is commonly known, at moderate pyrolysis temperatures, potassium (the second most important element in SM ash) promotes the production of char (Wang et al. 2010). The highest oil and tar yield with 36.02 wt% was characteristic for the pyrolysis of BSG. This result can be considered very promising at the process temperature of 773 K (Mohammed et al. 2016a). If the aqueous phase is considered, the total liquid mass for BSG has reached 61.27 wt%, while for MDF and SM it was 47.78 wt% and 51.45 wt%, respectively. Typically, the liquid phase of intermediate pyrolysis was ~40 wt% (Mohammed et al. 2016b). The gas phase yields were calculated from Eq. (15) for MDF, BSG, and SM. Both feedstocks, BSG and SM, have obtained about 11 wt% less gas yield compared to MDF. The increased pyrolysis gas yield of MDF was probably caused by the high cellulose content in the feedstock and the ash, which was particularly rich in

calcium, potassium, and sodium. In summary, the respective yields clearly depend on the type of feedstock used for the pyrolysis and its ash composition under the same process conditions.

### Composition of pyrolysis products

The composition of the pyrolysis gas is listed in Table 5. Nitrogen as a carrier was excluded from the gas composition, and only light gases detected by GC–MS are considered. The pyrolysis gas made of MDF turned out to be the most advantageous in terms of the content of combustible components. The only ballast component of the pyrolysis gas was carbon dioxide. The highest percentage of carbon dioxide was found in the gas formed from BSG; here, the ratio CO/CO<sub>2</sub> equals 1.4.

The higher heating value (HHV) of the combustible pyrolysis gas was calculated using Eq. (16),

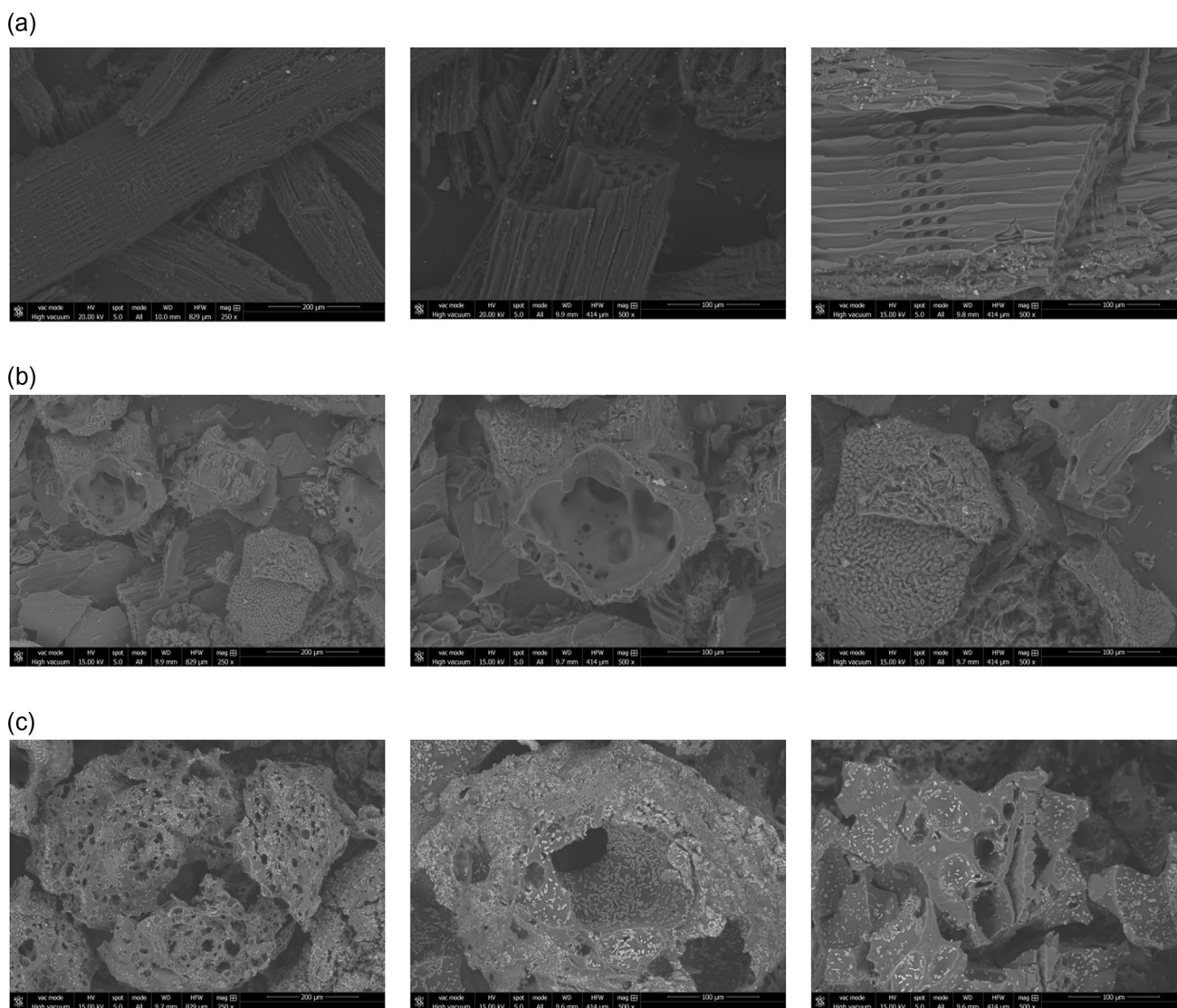
$$HHV_{\text{gas}} = \sum_{i=1}^n x_i \cdot HHV_i, \tag{16}$$

where  $x_i$  is mole fraction of the specific pyrolysis gas component,

$HHV_i$  is the higher heating value of the specific pyrolysis gas component.

The higher heating values of the selected pyrolysis gases applied in the calculation are listed in Table 6.

The calculated HHVs of the pyrolysis gases for MDF, BSG, and SM were 12049, 6619, and 8642 kJ/kg, respectively. The hydrogen content ranged from 9.28 to 11.55 vol%, which was satisfactory for a process temperature of 773 K.



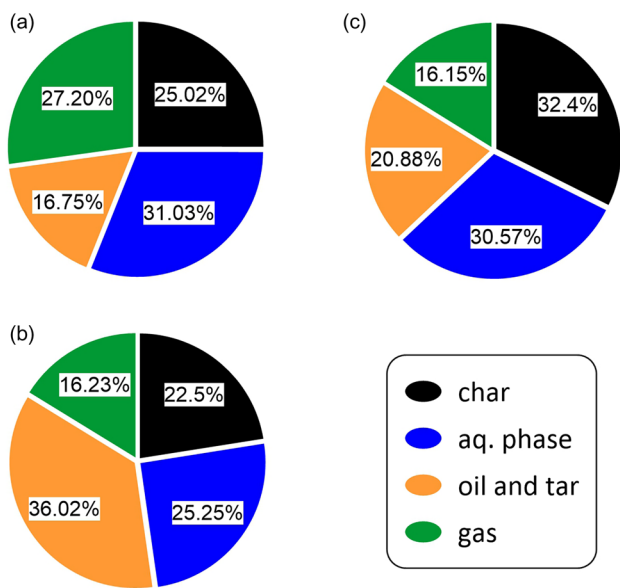
**Fig. 4** SEM micrographs of the chars obtained under pyrolysis: **a** MDF, **b** BSG, and **c** SM

Table 7 illustrates the results of the ultimate analyses for the char, oil, and the tar fraction and aqueous phase. As expected, the chars of MDF, BSG, and SM have exhibited a much higher carbon content and a lower percentage of hydrogen compared to the feedstocks (see Table 2). High carbon char after activation can be excellent catalysts for further applications in several industrial processes (Alaba et al. 2018). Importantly, MDF char contains the highest carbon content (73.8 wt%), although it had less carbon in the feedstock than BSG. This means that carbonisation of MDF was the most efficient. Only a slightly lower carbon content has been observed for BSG char (72.0 wt%). The carbon content of BSG char is satisfactory compared to the results of other scientists (Mahmood et al. 2013). Compared to this, the oxygen content is significantly reduced to levels below 20 wt% for the chars of MDF and BSG chars. Due to

the high oxygen content, SM char is unfavourable because it still contains 41 wt% O (that is, it is only reduced by 8 wt% compared to the raw material).

The second product group presented in Table 7 has covered oil and tar. The oil phase is targeted because it is easy to store and, after reducing the oxygen content, becomes an attractive fuel. About 51 wt% of carbon and 8 wt% of hydrogen were contained in MDF and SM tars and oils. The low oxygen content of 31.8 wt% is an unquestionable advantage of SM oil. The results of the ultimate analysis were similar to the oil produced from wood-derived materials by pyrolysis (Bridgwater 2018).

The last product of the intermediate pyrolysis process listed in Table 7 is the aqueous phase with a low carbon content (ranging from 12.8 wt% for SM to 14.9 wt% for



**Fig. 5** Pyrolysis product yields (weight basis) for **a** MDF, **b** BSG, and **c** SM

BSG). For all feedstocks used, similar hydrogen content in the aqueous phase (approximately 8 wt%).

**The heat balance of intermediate pyrolysis process**

The heat required for the pyrolysis of three biomass wastes was calculated based on Eqs. (1)–(13) and the data in Fig. 5, Tables 5 and 7, which was discussed previously. The results per 1 kg of feedstock are listed in Table 8. All  $Q_{py}$  values were positive, which means that all processes were endothermic. The estimated  $Q_{py}$  values of BSG, SM and MDF were + 881.09, + 1467.94, and + 2016.79 kJ, respectively. Although high-protein types of biomasses are not widely recommended for pyrolysis, our research shows that SM has a better energy balance than MDF boards. The heat required for pyrolysis was correlated with the  $K_2O/CaO$  ratio in the ash. The higher the  $K_2O/CaO$  ratio in biomass ash, the less heat was required for the pyrolysis process.  $Q_{py}$  can also be related to the yield of the pyrolysis products (Fig. 5). A positive correlation was found between the total oil and tar fraction as well as the char yield with  $Q_{py}$ (Fig. 6).

Interestingly, the following trend was observed for the present feedstocks: the higher the HHV value of the pyrolysis gas, the more heat was required for the pyrolysis process. This means that increasing the heat input during pyrolysis will improve yields and the resulting HHV of the pyrolysis gas. These results have demonstrated that the heat required for pyrolysis was dependent on the type of feedstock. For the three biomass wastes,  $Q_{py}$  for intermediate pyrolysis was slightly lower than for fast pyrolysis of forestry biomass at the same temperature (Fonts et al. 2021).

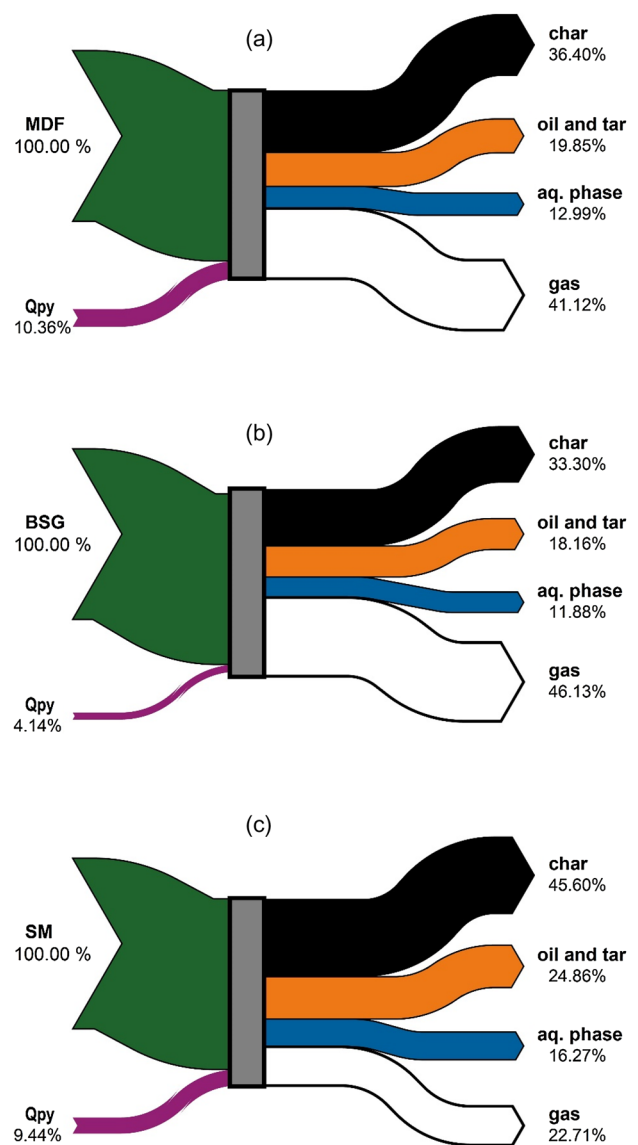


**Fig. 6** Sankey diagrams for **a** MDF, **b** BSG, and **c** SM pyrolysis (energy demand based on the relative share of HHV of the feedstock)

**Table 5** Pyrolysis gas composition obtained from MDF, BSG, and SM

Pyrolysis gas component	MDF	BSG	SM
CH <sub>4</sub> (vol%)	3.54	2.41	2.98
C <sub>2</sub> H <sub>6</sub> (vol%)	0	0.26	0.16
C <sub>2</sub> H <sub>4</sub> (vol%)	0	0.47	0.60
C <sub>2</sub> H <sub>2</sub> (vol%)	0	0.05	0.62
i-C <sub>4</sub> H <sub>10</sub> (vol%)	0	0	0.13
H <sub>2</sub> (vol%)	11.55	9.28	10.23
CO <sub>2</sub> (vol%)	2.14	36.43	24.78
CO (vol%)	82.76	51.10	60.46

**Table 6** Higher heating value constants for gases (Linstrom, PJ. and Mallard, WG. 2003)

Gas	HHV (kJ/mol)
CH <sub>4</sub>	890.7
C <sub>2</sub> H <sub>6</sub>	1560.7
C <sub>2</sub> H <sub>4</sub>	1411.2
C <sub>2</sub> H <sub>2</sub>	1300.4
i-C <sub>4</sub> H <sub>10</sub>	2869.0
H <sub>2</sub>	286.0
CO	283.2

The heat required for pyrolysis of biomass waste was also compared to the higher heating value intrinsically contained in the feedstock, here the  $Q_{py}$  values have ranged from 4.1–10.4% of higher heating value of the dry feedstock was missing to achieve self-sustaining energy of the pyrolysis process. The estimated  $Q_{py}$  is in line with values reported by (Ábrego et al. 2019) (3–15% HHV of biomass) and reported by (Crombie and Mašek 2014) (6–15% HHV of biomass).

The energy yields of char were significantly higher (36.40–45.60 wt%) than those of bio-oil (19.85–24.86 wt%), aqueous phase (11.88–16.27 wt%) and pyrolysis gas (22.71–41.12 wt%). These results were similar to the energy distribution of the pyrolysis of Bambara groundnut waste (Mohammed et al. 2017a).

## Conclusions

The studied biomass wastes were thermally converted via intermediate pyrolysis at 773 K confirming that this method can be applied successfully for various feedstocks and that energetically valuable products can be obtained. MDF and BSG were characterized as typical lignocellulosic materials but with remarkable differences in the contents of cellulose, hemicellulose, and lignin. The char yields of these

**Table 8** Balance of enthalpy of the investigated biomass wastes

Feedstock	MDF	BSG	SM
Standard enthalpy (kJ/kg feed)			
$H_{feed}^0$	-615.27	-744.18	-1738.97
$H_{oil}^0$	-974.07	-2356.43	-1485.45
$H_{aq,phase}^0$	-3137.12	-2491.69	-3213.04
$H_{gas}^0$	-1124.30	-1061.65	-923.66
Enthalpy change (kJ/kg feed)			
$\Delta H_{feed}$	0	0	0
$\Delta H_{char}$	155.09	139.47	200.83
$\Delta H_{oil}$	197.32	424.32	245.97
$\Delta H_{aq,phase}$	325.74	265.07	320.91
$\Delta H_{gas}$	158.58	87.35	90.62
Enthalpy (kJ/kg feed)			
$H_{N_2,in}$	0	0	0
$H_{feed}$	-6450.24	-6038.26	-7390.15
$H_{N_2,out}$	580.588	580.588	580.588
$H_{char}$	-460.18	-604.71	-1538.14
$H_{oil}$	-776.76	-1932.11	-1239.48
$H_{aq,phase}$	-2811.38	-2226.63	-2892.13
$H_{gas}$	-965.72	-974.30	-833.04
$Q_{py}$	2016.79	881.09	1467.94

two feedstocks were similar with very high carbon content (more than 70 wt%) and a correspondingly high calorific value. The pyrolysis of BSG resulted in the highest oil content (36.02 wt%), with 47.7 wt% C, 8.9 wt% H and a relatively low oxygen content, which is highly desirable. SM, which contains a dominating share of proteins, has been shown to be suitable for char production. In addition to char and oil, the aqueous phase was produced during pyrolysis. This kind of product has exhibited more than 10 wt% of carbon, consequently it may be applied in the production of

**Table 7** Ultimate analysis of the pyrolysis products of char, oil and aqueous phase

Parameter	Char			Oil and tar			Aqueous phase		
	MDF	BSG	SM	MDF	BSG	SM	MDF	BSG	SM
C (wt%)	73.78	72.02	49.67	51.18	47.71	50.99	14.16	14.92	12.77
H (wt%)	3.87	3.96	2.89	7.72	8.9	8.56	9.22	8.72	9.17
N (wt%)	3.66	6.35	6.45	4.06	4.56	8.68	3.00	2.31	5.52
O <sup>a</sup> (wt%)	18.69	17.67	40.99	37.07	38.33	31.77	73.62	74.05	72.54
H/C molar ratio	0.62	0.66	0.69	1.80	2.22	2.00	7.76	6.96	8.56
O/C molar ratio	0.19	0.18	0.62	0.54	0.61	0.47	3.90	3.73	4.26
N/C molar ratio $\times 10^{-2}$	4.24	7.56	11.13	6.80	8.20	14.60	18.17	13.28	37.06
Empirical formula	CH <sub>0.62</sub> O <sub>0.19</sub>	CH <sub>0.66</sub> O <sub>0.18</sub>	CH <sub>0.69</sub> O <sub>0.62</sub>	CH <sub>1.8</sub> O <sub>0.54</sub>	CH <sub>2.22</sub> O <sub>0.61</sub>	CH <sub>2.0</sub> O <sub>0.47</sub>	CH <sub>7.76</sub> O <sub>3.90</sub>	CH <sub>6.96</sub> O <sub>3.73</sub>	CH <sub>8.56</sub> O <sub>4.26</sub>
Formula weight (g/mol)	15.68	15.62	22.62	22.51	24.03	21.51	82.27	78.64	88.86
HHV (kJ/g)	28.33	27.89	16.41	23.08	23.06	24.47	8.15	7.79	7.70

<sup>a</sup>By difference



chemicals. The detailed analysis of feedstock ash composition allowed to investigate its influence on product yields. It was confirmed that potassium has promoted higher char production in the case of SM. The high content of CaO in MDF and SM could influence the formation of the pore structure in the corresponding char. In conclusion, the intermediate pyrolysis can be applied for lignocellulosic and high protein biomass, resulting in a high quality of char and oil as well as by-products for chemicals industry.

On the basis of the enthalpy balance, it was verified that the intermediate pyrolysis of the three biomass wastes was an endothermic process. The feedstock of BSG turned out to have the lowest energy demand in intermediate pyrolysis. A pyrolysis of BSG has required an additional heat input of + 881.1 kJ/kg (dry feed). Compared to this, an energy supply of + 2016.8 kJ/kg (dry feed) was assigned to the pyrolysis of MDF. Furthermore, it has been shown that the heat required for pyrolysis was correlated not only with the  $K_2O/CaO$  ratio in the ash but also with the yield of pyrolysis products. The heat required for pyrolysis was reduced as the  $K_2O/CaO$  ratio in biomass ash increases. There was also a tendency to reduce the heat required for pyrolysis as the total yield of char and oils increased. Thus, the pyrolysis reactions have required an additional energy input ranging from 4.14 to 10.36% of the HHV depending on the particular feedstock.

**Acknowledgements** This research project was supported by the program, “Excellence initiative—research university”, of the AGH University of Science and Technology (Grant AGH No. 501.696.7996). Part of this work was financed by the Polish National Agency for Academic Exchange (NAWA, Exchange programme for students and scientists as a part of bilateral cooperation, grant no. PPN/BIL/2018/1/00027) jointly with the German Academic Exchange Service (DAAD, Grant No. 57448108)

**Authors' contributions** WJ: Conceptualisation, methodology, writing the original draft, data curation, and investigation. AM: Project administration, funding acquisition, writing, review, editing, and investigation. MR: Writing, review, editing, and investigation.

**Data availability** The datasets generated and/or analysed during this study are available from the corresponding author on reasonable request.

## Declarations

**Conflict of interest** The authors declare that they have no conflicts of interest.

**Open Access** This article is licensed under a Creative Commons Attribution 4.0 International License, which permits use, sharing, adaptation, distribution and reproduction in any medium or format, as long as you give appropriate credit to the original author(s) and the source, provide a link to the Creative Commons licence, and indicate if changes were made. The images or other third party material in this article are included in the article's Creative Commons licence, unless indicated otherwise in a credit line to the material. If material is not included in

the article's Creative Commons licence and your intended use is not permitted by statutory regulation or exceeds the permitted use, you will need to obtain permission directly from the copyright holder. To view a copy of this licence, visit <http://creativecommons.org/licenses/by/4.0/>.

## References

- Ábrego J, Atienza-Martínez M, Plou F, Arauzo J (2019) Heat requirement for fixed bed pyrolysis of beechwood chips. *Energy* 178:145–157. <https://doi.org/10.1016/j.energy.2019.04.078>
- Alaba PA, Abbas A, Huang J, Daud WMAW (2018) Molybdenum carbide nanoparticle: Understanding the surface properties and reaction mechanism for energy production towards a sustainable future. *Renew Sustain Energy Rev* 91:287–300. <https://doi.org/10.1016/j.rser.2018.03.106>
- Alper K, Tekin K, Karagöz S (2015) Pyrolysis of agricultural residues for bio-oil production. *Clean Technol Environ Policy* 17:211–223. <https://doi.org/10.1007/s10098-014-0778-8>
- Atsonios K, Panopoulos KD, Bridgwater AV, Kakaras E (2015) Biomass fast pyrolysis energy balance of a 1kg/h test rig. *Int J Thermodyn* 18:267–275. <https://doi.org/10.5541/ijot.5000147483>
- Bertero M, Sedran U (2015) Recent Advances in Thermochemical Conversion of Biomass, Chapter 13—Coproducting of Bio-oil in Fluid Catalytic Cracking. Elsevier B.V.
- Borel LDMS, Lira TS, Ribeiro JA et al (2018) Pyrolysis of brewer's spent grain: kinetic study and products identification. *Ind Crops Prod* 121:388–395. <https://doi.org/10.1016/j.indcrop.2018.05.051>
- Bridgwater T (2018) Challenges and opportunities in fast pyrolysis of biomass: Part II. *Johnson Matthey Technol Rev* 62:150–160. <https://doi.org/10.1595/205651318X696738>
- Bridgwater AV (2012) Review of fast pyrolysis of biomass and product upgrading. *Biomass Bioenergy* 38:68–94. <https://doi.org/10.1016/j.biombioe.2011.01.048>
- Cancelliere R, Carbone K, Pagano M et al (2019) Biochar from brewers' spent grain: a green and low-cost smart material to modify screen-printed electrodes. *Biosensors* 9. <https://doi.org/10.3390/bios9040139>
- Channiwala SA, Parikh PP (2002) A unified correlation for estimating HHV of solid, liquid and gaseous fuels. *Fuel* 81:1051–1063. [https://doi.org/10.1016/S0016-2361\(01\)00131-4](https://doi.org/10.1016/S0016-2361(01)00131-4)
- Chen D, Cen K, Zhuang X et al (2022) Insight into biomass pyrolysis mechanism based on cellulose, hemicellulose, and lignin: Evolution of volatiles and kinetics, elucidation of reaction pathways, and characterization of gas, biochar and bio-oil. *Combust Flame* 242. <https://doi.org/10.1016/j.combustflame.2022.112142>
- Chen M, Zhang Y, Li Y et al (2020) Soybean meal-based wood adhesive enhanced by phenol hydroxymethylated tannin oligomer for exterior use. *Polymers (basel)* 12. <https://doi.org/10.3390/POLYM12040758>
- Chen NY, Walsh DE, Koenig LR (1988) Fluidized-bed upgrading of wood pyrolysis liquids and related compounds. *ACS Symp Ser* 277–289. <https://doi.org/10.1021/bk-1988-0376.ch024>
- Chen Q, Yang R, Zhao B et al (2014) Investigation of heat of biomass pyrolysis and secondary reactions by simultaneous thermogravimetry and differential scanning calorimetry. *Fuel* 134:467–476. <https://doi.org/10.1016/j.fuel.2014.05.092>
- Chong YY, Thangalazhy-Gopakumar S, Ng HK et al (2019) Catalytic pyrolysis of cellulose with oxides: effects on physical properties and reaction pathways. *Clean Technol Environ Policy* 21:1629–1643. <https://doi.org/10.1007/s10098-019-01737-6>
- Cong H, Mašek O, Zhao L et al (2018) Slow pyrolysis performance and energy balance of corn stover in continuous pyrolysis-based



- poly-generation systems. *Energy Fuels* 32:3743–3750. <https://doi.org/10.1021/acs.energyfuels.7b03175>
- Couret L, Irle M, Belloncle C, Cathala B (2017) Extraction and characterization of cellulose nanocrystals from post-consumer wood fiberboard waste. *Cellulose* 24:2125–2137. <https://doi.org/10.1007/s10570-017-1252-7>
- Crombie K, Mašek O (2014) Investigating the potential for a self-sustaining slow pyrolysis system under varying operating conditions. *Bioresour Technol* 162:148–156. <https://doi.org/10.1016/j.biortech.2014.03.134>
- Dahou T, Defoort F, Khiari B et al (2021) Role of inorganics on the biomass char gasification reactivity: A review involving reaction mechanisms and kinetics models. *Renew Sustain Energy Rev* 135. <https://doi.org/10.1016/j.rser.2020.110136>
- Daugaard DE, Brown RC (2003) Enthalpy for pyrolysis for several types of biomass. *Energy Fuels* 17:934–939. <https://doi.org/10.1021/ef020260x>
- El-Hendawy ANA (2006) Variation in the FTIR spectra of a biomass under impregnation, carbonization and oxidation conditions. *J Anal Appl Pyrolysis* 75:159–166. <https://doi.org/10.1016/j.jaap.2005.05.004>
- Ferreira SD, Altafini CR, Perondi D, Godinho M (2015) Pyrolysis of medium density fiberboard (MDF) wastes in a screw reactor. *Energy Convers Manag* 92:223–233. <https://doi.org/10.1016/j.enconman.2014.12.032>
- Fonts I, Atienza-Martínez M, Carstensen HH et al (2021) Thermodynamic and physical property estimation of compounds derived from the fast pyrolysis of Lignocellulosic materials. *Energy Fuels* 35:17114–17137. <https://doi.org/10.1021/acs.energyfuels.1c01709>
- Funke A, Tomasi Morgano M, Dahmen N, Leibold H (2017) Experimental comparison of two bench scale units for fast and intermediate pyrolysis. *J Anal Appl Pyrolysis* 124:504–514. <https://doi.org/10.1016/j.jaap.2016.12.033>
- Gomez C, Velo E, Barontini F, Cozzani V (2009) Influence of pressure on the heat of biomass pyrolysis. *Ind Eng Chem Res* 48:10222–10233. <https://doi.org/10.1021/ie9007985>
- Gonultas O, Candan Z (2018) Chemical characterization and fir spectroscopy of thermally compressed eucalyptus wood panels. *Maderas Cienc y Tecnol* 20:431–442. <https://doi.org/10.4067/S0718-221X2018005031301>
- Grieshop CM, Kadzere CT, Clapper GM et al (2003) Chemical and nutritional characteristics of United States soybeans and soybean meals. *J Agric Food Chem* 51:7684–7691. <https://doi.org/10.1021/jf034690c>
- Haseli Y, Van Oijen JA, De Goey LPH (2011) Modeling biomass particle pyrolysis with temperature-dependent heat of reactions. *J Anal Appl Pyrolysis* 90:140–154. <https://doi.org/10.1016/j.jaap.2010.11.006>
- Hoekstra E, Westerhof RJM, Brilman W et al (2012) Heterogeneous and homogeneous reactions of pyrolysis vapors from pine wood. *AIChE J* 58:2830–2842. <https://doi.org/10.1002/aic.12799>
- Hornung A (2013) Intermediate pyrolysis of biomass. In: *Biomass Combustion Science*. Technol Eng, pp 172–186
- Hosokai S, Matsuoka K, Kuramoto K, Suzuki Y (2016) Practical estimation of reaction heat during the pyrolysis of cedar wood. *Fuel Process Technol* 154:156–162. <https://doi.org/10.1016/j.fuproc.2016.08.027>
- Jerzak W, Bieniek A, Magdziarz A (2022) Multifaceted analysis of products from the intermediate co-pyrolysis of biomass with Tetra Pak waste. *Int J Hydrogen Energy*. Doi: <https://doi.org/10.1016/j.ijhydene.2021.06.202>
- Kodera Y, Kaiho M (2016) model calculation of heat balance of wood pyrolysis. *J Japan Inst Energy* 95:881–889. <https://doi.org/10.3775/jie.95.881>
- Li X, Wei Y, Xu J et al (2018) Quantitative visualization of lignocellulose components in transverse sections of moso bamboo based on fir macro- and micro-spectroscopy coupled with chemometrics. *Biotechnol Biofuels* 11:1–16. <https://doi.org/10.1186/s13068-018-1251-4>
- Linstrom, PJ., Mallard, WG. (2003) Nist standard reference database number 69. In: NIST Chem. Webb. <http://webbook.nist.gov>
- Mahmood ASN, Brammer JG, Hornung A et al (2013) The intermediate pyrolysis and catalytic steam reforming of brewers spent grain. *J Anal Appl Pyrolysis* 103:328–342. <https://doi.org/10.1016/j.jaap.2012.09.009>
- Mašek O (2016) Biochar in thermal and thermochemical biorefineries-production of biochar as a coproduct. *Handb Biofuels Prod Process Technol Second Ed* 655–671. <https://doi.org/10.1016/B978-0-08-100455-5.00021-7>
- Mohammed IY, Abakr YA, Musa M et al (2016a) Valorization of Bambara groundnut shell via intermediate pyrolysis: Products distribution and characterization. *J Clean Prod* 139:717–728. <https://doi.org/10.1016/j.jclepro.2016.08.090>
- Mohammed IY, Abakr YA, Xing Hui JN et al (2017a) Recovery of clean energy precursors from Bambara groundnut waste via pyrolysis: Kinetics, products distribution and optimisation using response surface methodology. *J Clean Prod* 164:1430–1445. <https://doi.org/10.1016/j.jclepro.2017.07.068>
- Mohammed IY, Abakr YA, Yusup S et al (2017b) Upgrading of Napier grass pyrolytic oil using microporous and hierarchical mesoporous zeolites: products distribution, composition and reaction pathways. *J Clean Prod* 162:817–829. <https://doi.org/10.1016/j.jclepro.2017.06.105>
- Mohammed IY, Kazi FK, Yusup S et al (2016b) Catalytic intermediate pyrolysis of Napier grass in a fixed bed reactor with ZSM-5, HZSM-5 and zinc-exchanged zeolite-a as the catalyst. *Energies* 9. <https://doi.org/10.3390/en9040246>
- Mohammed IY, Lim CH, Kazi FK et al (2017c) Co-pyrolysis of rice husk with underutilized biomass species: a sustainable route for production of precursors for fuels and valuable chemicals. *Waste and Biomass Valorization* 8:911–921. <https://doi.org/10.1007/s12649-016-9599-9>
- Morgan TJ, Kandiyoti R (2014) Pyrolysis of coals and biomass: analysis of thermal breakdown and its products. *Chem Rev* 114:1547–1607. <https://doi.org/10.1021/cr400194p>
- Oliveira TJP, Cardoso CR, Ataíde CH (2015) Fast pyrolysis of soybean hulls: analysis of bio-oil produced in a fluidized bed reactor and of vapor obtained in analytical pyrolysis. *J Therm Anal Calorim* 120:427–438. <https://doi.org/10.1007/s10973-015-4600-6>
- Pan L, Jiang Y (2019) Evaluating the effects of KCl on thermal behavior and reaction kinetics of medium density fiberboard pyrolysis. *Materials (basel)* 12:1826. <https://doi.org/10.3390/ma12111826>
- Patwardhan PR, Satrio JA, Brown RC, Shanks BH (2010) Influence of inorganic salts on the primary pyrolysis products of cellulose. *Bioresour Technol* 101:4646–4655. <https://doi.org/10.1016/j.biortech.2010.01.112>
- Sun Y, Li C, Zhang S et al (2021) Pyrolysis of soybean residue: understanding characteristics of the products. *Renew Energy* 174:487–500
- Van Soest PJ (1963) Use of Detergents in the analysis of fibrous feeds. II. A Rapid method for the determination of fiber and lignin. *J Assoc Off Agric Chem* 46:829–835
- Vassilev SV, Baxter D, Andersen LK, Vassileva CG (2010) An overview of the chemical composition of biomass. *Fuel* 89:913–933. <https://doi.org/10.1016/j.fuel.2009.10.022>
- Wang F, Zheng Y, Zhai Q et al (2020) Catalytic co-pyrolysis of Yunnan pine and hydrogen donor over desilicated ZSM-5 for light aromatics. *Int J Hydrogen Energy* 45:26929–26937. <https://doi.org/10.1016/j.ijhydene.2020.05.235>

- Wang Z, Wang F, Cao J, Wang J (2010) Pyrolysis of pine wood in a slowly heating fixed-bed reactor: potassium carbonate versus calcium hydroxide as a catalyst. *Fuel Process Technol* 91:942–950. <https://doi.org/10.1016/j.fuproc.2009.09.015>
- Xiros C, Topakas E, Katapodis P, Christakopoulos P (2008) Hydrolysis and fermentation of brewer's spent grain by *Neurospora crassa*. *Bioresour Technol* 99:5427–5435. <https://doi.org/10.1016/j.biortech.2007.11.010>
- Yang H, Kudo S, Kuo HP et al (2013) Estimation of enthalpy of bio-oil vapor and heat required for pyrolysis of biomass. *Energy Fuels* 27:2675–2686. <https://doi.org/10.1021/ef400199z>
- Yang H, Yan R, Chen H et al (2007) Characteristics of hemicellulose, cellulose and lignin pyrolysis. *Fuel* 86:1781–1788. <https://doi.org/10.1016/j.fuel.2006.12.013>
- Yang Q, Zhou H, Bartocci P et al (2021) Prospective contributions of biomass pyrolysis to China's 2050 carbon reduction and renewable energy goals. *Nat Commun* 12:1–12. <https://doi.org/10.1038/s41467-021-21868-z>
- Zazycki MA, Perondi D, Godinho M et al (2020) Conversion of MDF wastes into a char with remarkable potential to remove Food Red 17 dye from aqueous effluents. *Chemosphere* 250. <https://doi.org/10.1016/j.chemosphere.2020.126248>
- Zhang H, Cheng YT, Vispute TP et al (2011) Catalytic conversion of biomass-derived feedstocks into olefins and aromatics with ZSM-5: the hydrogen to carbon effective ratio. *Energy Environ Sci* 4:2297–2307. <https://doi.org/10.1039/c1ee01230d>
- Zhang S, Wang J, Zhu S et al (2020) Effects of MgCl<sub>2</sub> and Mg(NO<sub>3</sub>)<sub>2</sub> loading on catalytic pyrolysis of sawdust for bio-oil and MgO-impregnated biochar production. *J Anal Appl Pyrolysis* 152. <https://doi.org/10.1016/j.jaap.2020.104962>

**Publisher's Note** Springer Nature remains neutral with regard to jurisdictional claims in published maps and institutional affiliations.

## Authors and Affiliations

Wojciech Jerzak<sup>1</sup>  · Markus Reinmüller<sup>2,3</sup> · Aneta Magdziarz<sup>1</sup>

<sup>1</sup> AGH University of Science and Technology, Mickiewicza 30 Av., 30-059 Krakow, Poland

<sup>2</sup> Institute of Energy Process Engineering and Chemical Engineering, Technische Universität Bergakademie Freiberg, Fuchsmühlenweg 9 D (Reiche Zeche), 09599 Freiberg, Germany

<sup>3</sup> DTU Engineering Technology, Technical University of Denmark, Lautrupvang 15, 2750 Ballerup, Denmark